Iraqi Journal of Science, 2025, Vol. 66, No. 10, pp: 4113- 4136
DOI: 10.24996/ijs.2025.66.10.9

ISSN: 0067-2904

Employment of a Silica Gel Formulated from Steel Slag to Remove Lead, Nickel and Cadmium in Aqueous Solution

Toufik Chouchane*[1], Atmane Boukari[1], Sabiha. Chouchane[2], Ouahida Khireddine[1], Mohamed T. Abedghars [1], Hazem Meradi[1]

[1] *Research Center in Industrial Technologies CRTI, P.O. Box 64, Cheraga 16014 Algiers Algeria*
[2]*Faculty of Sciences, Badji Mokhtar University, Annaba Algeria*

Received: 10/12/2024 Accepted: 24/7/2025 Published: 30/10/2025

Abstract

In this study, silica gel (SG) derived from steel slag (SS) was utilized as an adsorbent for the removal process of lead, nickel and cadmium, both individually and in combination. Experimental results demonstrated that steel slag was successfully converted into silica gel by chemical and thermal treatments, yielding a material composed of 95.61% silica with a specific surface area of 472.38 m^2/g. Monitoring of adsorption processes highlighted the considerable impact of contact time, pH, temperature, stirring speed, and initial concentration on these processes. The amounts absorbed after 50 minutes of contact for lead, nickel, and cadmium were 144.74, 133.14 and 126.89 mg/g. However, for the mixture, it had reached 119.12 mg/g after 70 minutes of agitation. Adsorption isotherms demonstrated that the adsorption of the ions examined occurs on a homogeneous monolayer surface. The separation factor (R_L) and intensity of sorption (1/n) showed that the processes performed were favorable. Kinetic analysis revealed that the adsorption processes followed pseudo-second-order kinetics, depending on both external and internal diffusion. Thermodynamically, the processes were found to be exothermic, spontaneous, and less entropic. The values change in free energy, enthalpy variation, and Temkin constant (b_T) have shown that these processes were characterized by adsorption of a physical nature.

Keywords. Adsorption kinetics, Toxic metals, Slag, Silica gel, Adsorption isotherm

1. Introduction

The contamination of water resources by hazardous inputs toxic elements, particularly toxic metals, has emerged as a significant issue impacting rich and developing countries. Indeed, they constitute a permanent threat to the health of living organisms and jeopardize the conservation of animal and plant species [1]. In response to this concerning situation, various decontamination techniques such as membrane processes (ultrafiltration, nanofiltration, and reverse osmosis), physicochemical methods (chemical precipitation, coagulation-flocculation, decantation, filtration, and ion exchanges), as well as adsorption have been developed and implemented [2]. For this project, the adsorption process was selected due to its reliability, high efficiency, cost-effectiveness, and minimal sludge production [2]. The pollutants selected are lead, nickel, and cadmium. The adsorbent studied is silica gel synthesized from a steel by-product, namely blast furnace slag.

*Email: chouchane_toufik@yahoo.fr

Lead, cadmium, and nickel are harmful elements capable of representing a significant danger to humans and their environment due to their non-degradable, durable, and accumulative nature [3]. Lead, even at minimal concentrations, is capable of causing severe infections in the digestive system, damaging cell membranes, and causing problems in the nerves and kidneys [2,3]. Lead contamination is mainly caused by mining, activities in the steel and metallurgical sectors, corrosion of lead pipes, storage of lead-acid batteries, and electronic waste [2]. Nickel can cause liver damage, atopic eczema, kidney problems, hair loss, headaches, dizziness, and chest pain [4]. The main sources of pollution are the steel and metaallurgical industries, as well as thermal power plants and battery production [5]. Cadmium also has toxic and harmful effects. It can cause severe nerve and kidney damage while potentially damaging proteins, lipids, and DNA through the formation of free radicals in the body [6]. Cadmium pollution is mainly due to zinc smelting, used batteries, electronic waste, paint residues, incineration, and fuel combustion operations [7]. Given this serious threat, extensive research has focused on removing these hazardous from wastewater. Literature reports indicate that the elimination of lead, nickel, and cadmium in solution has been carried out by adsorption using different adsorbents, such as clays and their derivatives, steel co-products and their derivatives, and elements from wood, as summarized in Table 1.

According to T. Chouchane et al. [2,4], the efficient removal of nickel and lead by physical adsorption on blast furnace slag, in static mode, was achieved on a homogeneous monolayer surface, taking into account determining factors. They also specify that the maximum adsorption capacities reached 53.58 mg/g after 90 minutes of contact for nickel and 34.26 mg/g after 50 minutes of stirring for lead. Liu et al. [8] demonstrated that the removal process of Pb(II), Cd(II), and Ni(II) in a ternary mixture using porous geopolymer foams of phosphoric origin seems both feasible and efficient at pH 7, where the selectivity order of the adsorbed metals was Pb(II) > Ni(II) > Cd(II). They also explain that the adsorption mechanism of the heavy metals examined is shared between ion exchange and surface complexation. On the other hand, Peng et al. [9] showed that the adsorption of Pb(II), Cd(II), and Ni(II) in a ternary mixture by modified sulfonated graphene oxide was efficiently performed on a homogeneous monolayer surface at pH 6, where the selectivity order is Pb(II) > Cd(II) > Ni(II). Moreover, their results highlighted that the majority of the adsorption occurred during the first 15 min, while equilibrium was established after 60 min. Khan et al. [10] reported that the adsorption of Pb(II) and Ni(II) onto TiO_2 nanoparticles was favorable, exhibited endothermic behavior, and occurred spontaneously. Furthermore, they found that the adsorption process relies on several factors, such as contact time, pH, temperature, ionic strength, humic acid, and foreign ions, also concluding that lead (40 mg/g) was adsorbed more efficiently than nickel (26.32 mg/g).

Table 1: Adsorbents used for the removal of lead, nickel and cadmium

Element	Adsorbent	Reference
Lead	Cocoa (Theobroma Cacao L)	[3]
	BFS	[2]
	Porous geopolymer foams	[8]
	Modified sulfonated graphene	[9]
	Carbon nanomaterial-based aerogels	[10]
	TiO_2nanoparticles	[11]
Nickel	Cocoa (Theobroma Cacao L)	[3]
	BFS	[4]
	Magnetite rich clay	[5]
	Porous geopolymer foams	[8]
	Modified sulfonated graphene	[9]
	TiO_2 nanoparticles	[11]
	Jourdan natural zeolite	[12]
	Biochar	[13]
Cadmium	Modified Blast Furnace Slag	[6]
	Porous geopolymer foams	[10]
	Modified sulfonated graphene	[9]
	Biochar	[13]
	Modified pine wood sawdust	[14]
	Halloysite	[15]

The slag from the blast furnace, which is the basic material of the new synthesized adsorbent, comes from the cast iron manufacturing process. It is basically formed of lime, silica, alumina, magnesium oxide, and traces of metal ion oxides, namely iron oxide, manganese oxide, potassium oxide, and sodium oxide. It has proven to be a reliable and efficient adsorbent in the field of water decontamination, especially for the adsorption of toxic metals such as lead [2], nickel [4], cadmium [6], and cobalt [16]. Additionally, it has been utilized for the adsorption of dyes, especially acidic methyl orange [17], and acid dye [18]. According to the literature, materials from blast furnace slag have also established themselves as reliable, efficient, and competitive adsorbents in the processes of removing harmful elements in solution. Indeed, it has been reported in several recent scientific publications that blast furnace slag has been efficiently transformed into high-performance adsorbent materials. Among these materials generated, it has been mentioned:

- The hydroxyapatite-zeolite synthesized from slag was applied in the adsorption process of Cd^{+2} ions. This study revealed that the adsorption was carried out on a homogeneous monolayer surface and followed pseudo-second-order kinetics. Moreover, it was reported that the adsorption capacity reached 133.34 mg/g at 20 °C under the effects of electrostatic interactions [6].
- The hydroxyapatite-zeolite synthesized from slag after 6 hours of ageing was used in the adsorption process of Mn^{2+}, NH^{4+}, and PO_4^{3-} ions [19], where it was noted that the adsorption processes carried out were accomplished efficiently. For 50 mg/L solutions, the measured adsorption values were 25.98 mg/g for Mn^{2+}, 20.10 mg/g for NH^{4+}, and 26.41 mg/g for PO_4^{3-}, respectively [19].

- Silica nanoparticles, obtained from blast furnace slag, were used for the removal of methylene blue from an aqueous solution. The results of this expertise showed that the adsorption was favorable and maximal at pH 8, with a maximum adsorption capacity of 109.8 mg/g [20].
- The obtained oxalated slag was used for the removal of Co^{2+} in solution. The results showed that the adsorption capacity, after transformation, increased from 113 mg/g to 576 mg/g, which was estimated as a high performance [21]. Moreover, its efficiency in the adsorption of cesium and strontium ions from multimetallic aqueous solutions was reported [21].
- Na-A zeolite prepared from blast furnace slag was used as an adsorbent for the removal of methylene blue from aqueous solution. The results demonstrated that the adsorption is favorable and follows pseudo-second-order kinetics, with an adsorption capacity of 21.89 mg/g [22].
- Zeolite obtained from blast furnace slag was used as an adsorbent to remove copper and cadmium from aqueous solution. This study revealed that the adsorption process was extremely rapid, allowing the removal of more than 99% of both metals within 10 minutes, while complete removal was achieved within 20 minutes. The measured adsorption capacities were 103 mg/g for copper and 80 mg/g for cadmium [23].
- Porous geopolymer was developed using titanium-containing blast furnace slag. This study revealed that this material performs two functions, namely adsorption and photocatalytic degradation, thus providing a promising solution for dye removal [24].

This study investigates the conversion of blast furnace slag into silica gel for use as a cost-effective and efficient adsorbent for the suppression of heavy metals, notably lead, nickel, and cadmium, which are either separately or in a mixture, thus allowing its valorization in the sector of treatment of water contaminated by metallic pollutants. The focus on silica gel synthesis is due to its high porosity and high specific surface area, which make it a reliable and efficient product [25]. Indeed, silica gel has been effectively used to treat water, removing pollutants and performing desalination. For example, it has been used for the removal of acephalous pesticides by photocatalytic degradation [26]. In addition, it has been used to remove lead ions in solution through the adsorption process [27]. According to Woo et al. [28], it has been used in desalination and water cooling by adsorption.

Following characterization, the synthesized material was employed to remove selected pollutants via batch adsorption. The interactions between the pollutants and the adsorbent, the removal mechanism, and the nature of the processes were addressed. It should be emphasized that the influence of the determining parameters, namely the contact time, the particle size of the solid, the stirring speed, the pH of the solution, the temperature of the medium, and the initial concentration of the solute, was examined.

The treatment and conversion of SS to SG were accomplished following chemical and thermal treatments. The characterization of SS and SG was performed by X-ray fluorescence (XRF), X-ray diffraction (XRD), and energy dispersive spectroscopy (EDS). The specific surface area and pore volumes were determined by BET and BJH models. The contributions of Freundlich, Langmuir, and Temkin adsorption isotherms were crucial in understanding the interactions between SG and the pollutants studied. The Lagergren, Blanchard, and Weber Morris models made a positive contribution to the understanding of the adsorption kinetics. The Van Hoff equation and thermodynamic parameters allowed us to determine the nature of this process.

2. Materials and methods

2.1 Synthesis of silica gel

The slag from the blast furnace at the El-Hadjar steel complex in Algeria was processed following the experimental procedures described by de Chouchane et al. [2,4]. The subsequent synthesis of silica gel from treated blast furnace slag was accomplished according to the experimental protocol detailed below.

- 100 g of the treated slag was ground and sieved to particle sizes of around 1 mm
- A mixture of 50 g of treated slag and 100 mL of NaOH solution (0.1 M) were introduced into a beaker with a volume of 1 L.
- The new solid obtained from the mixture was heated at 800 °C for 2 hours in a muffle furnace after being previously stirred slowly at 100 rpm for 90 minutes. After cooling, 30 g of the resulting solid was incorporated into a 120 ml Na_2HPO_4 solution (10 mg/L). The new mixture was kept stirring until completely homogeneous.
- After standing for almost 8 hours, the solid was isolated by filtration and then subjected to evaporation to dryness, which allowed sodium metasilicate Na_2SiO_3 to be obtained as a residue. The undesirable substances, namely $Al(OH)_3$ and $Ca(OH)_2$, were eliminated by filtration following the standing and cooling of the solution. It is crucial to note that the quantities of lime and alumina were retained in the liquid phase following filtration. Before removing them, we first adjusted the pH to 10 to precipitate them, and then recovered them by filtration.
- 20 g of sodium metasilicate were dissolved in distilled water while being gently stirred at 100 rpm. After 30 minutes, 30 mL of 1 M H_2SO_4 was added dropwise to induce silica gel formation. It is worth mentioning that sodium sulfate (Na_2SO_4) was removed by the gradual addition of deionized water.
- The resulting gel was washed, baked at 105°C for 8 hours, heated in a muffle furnace at 600°C for 120 minutes, and cooled for 2 hours before being ground and stored in flasks. It is worth noting that for 20 g of sodium metasilicate, we recovered 18.3 g of silica gel, representing a yield of approximately 91.5%.

2.2 Instruments and reagents

The Perkin Elmer 3110 atomic absorption spectrometer was used to analyze lead, nickel, and cadmium ions. Silica gel and treated slag were analyzed by XRF (Siemens SRS 3000, France), XRD (Rigaku Ultima IV, Germany), and EDS (Zeiss EVO MA25, Germany).The pH value was evaluated using a high-quality Ericsson pH meter. The heating operation of SG was carried out in a Nabertherm model HT16/17 muffle furnace. The grinding of SG was accomplished by a micro planetary mill (PULVERISETTE 7 premium line, France). Agitation of the solutions studied was performed by a mechanical stirrer operating at multiple speeds. The evaluation of the mass area, also referred to as specific surface area was measured thanks to the Brunauer, Emmett, and Teller model.

The reagents used, namely hydrochloric acid (HCl), sulfuric acid (H_2SO_4), sodium hydroxide (NaOH), nickel nitrate ($Ni(NO_3)_2 \cdot 6H_2O$), lead nitrate ($Pb(NO_3)_2$), and cadmium nitrate ($Cd(NO_3)_2 \cdot 4H_2O$), were of analytical grade (Merck). While sodium hydrogen phosphate (Na_2HPO_4) is from Haltichem. Blast furnace slag from the Annaba steel complex, Algeria.

2.3 Specific surface determination

The specific surface area was evaluated by measuring the amount of nitrogen absorbed, corresponding to the pressure to which it was subjected. This method is based on the principle of gas adsorption at low temperatures to determine the total surface area of a solid sample without

altering its structure. The Van der Waals forces at the surface of the solid are at the origin of this process, exerting their action on the gas molecules surrounding the solid sample. This experiment was carried out at a temperature of -196°C and under a pressure equivalent to the standard atmospheric pressure of 760 mmHg [6,0]. The specific surface area evaluation was carried out by nitrogen adsorption-desorption adopting the BET method, while the pore size was determined using the BJH method [8,13]. It is important to note that gas adsorption provides rapid and valuable information on the porosity of a sample, since the shape of the isotherm and the hysteresis already reveal the type of porosity and the configuration of the pores.

2.4 Point of Zero Charge

The specification of the point of zero charge (PZC) is of great importance because it provides information on the type of charge on the surface of the solid analyzed, whether positive, neutral, or negative. For this reason, we measured it in order to facilitate the understanding of the adsorption process. Based on the experiences of previously conducted research works [2,6], we evaluated the agreement of the pH to the PZC. For this experiment, 1 g of SG (200 µm particle size) was treated with 100 mL of KCl solution (0.1 M and 0.01 M) [4]. The solutions examined were stirred moderately (150 rpm) for 12 hours; the temperature of the medium examined varied between 20 and 25 °C. The pH was adjusted by sulfuric acid.

2.5 Adsorption process

A series of batch experiments was conducted to assess the adsorption of lead, nickel, and cadmium from aqueous solutions onto the SG. Nickel nitrate ($Ni(NO_3)_2 \cdot 6H_2O$), lead nitrate ($Pb(NO_3)_2$), and cadmium nitrate ($Cd(NO_3)_2 \cdot 4H_2O$) were used to prepare the lead, nickel and cadmium stock solutions. The volume of the solutions used is 1 liter. The experimental approach adopted is similar to the experimental method described in the literature [2,4,6]. The procedure of the experiment involved the addition of a defined amount of SG to a solution containing the pollutant(s) to be analyzed while following the protocol step by step until the results were obtained. Contact time (tc), particle sizes (Øs), stirring speed (V_{ag}), solution pH, initial concentration of the pollutant solution (C_0) and solution temperature (T) were essential factors for the accomplishment of this process; see Table 2. The mass of the adsorbent is 1 g in all the experiments carried out. The initial concentrations of the examined metallic pollutants (Pb(II), Ni(II), and Cd(II)) in the mixture are equivalent, and each concentration represents one third of the overall concentration (1/3 C_0). The pH of the solution was adjusted to the appropriate value with the addition of droplets of H_2SO_4 (0.05 M) and NaOH (0.05 M). It should be emphasized that the values of the suggested determining factors have been established from numerous experiments and based on reliable literary references [3,6,8,11].

The quantities indicating the efficiency of this process, namely the residual concentration at equilibrium (Ce, mg/L), the adsorbed quantity (qe, mg/g), as well as the adsorption percentage (R, %), were determined using equations 1, 2, and 3.

$$C_e = C_0 - C_t \quad (1)$$

$$q_e = \frac{C_0 - C_t}{m_s} \times V \quad (2)$$

$$R = \frac{C_0 - C_e}{C_0} \times 100 \quad (3)$$

Where C_0= starting concentration (mg/L), C_t= concentration measured at time t (mg/L), C_e= concentration measured at equilibrium (mg/L), m_s= mass of the adsorbent (g), and V= volume of the solution (1L).

Table 2: Detailed specifications for each stage of the experiment

Steps	Parameter values
Impact of t_c	t_c: 0-300 min (element alone and in mixture), Øs: 200 µm, V_{ag}: 100 rpm; T: 20 °C; pH: 4.2; C_0: 60 mg/L, ms: 1 g, Δt: ±5 s
Impact of Øs	t_c: 50 min (alone) ; t_c: 70 min (mixture); Øs: 50, 100, 150, 200, 300, and 400 µm, V_{ag}: 100 rpm; T : 20 °C, pH: 4.2; C_0: 60 mg/L, ms: 1 g, ΔØs: ±0.1 µm
Impact of V_{ag}	t_c: 50 min (alone) ; t_c: 70 min (mixture); Øs: 200 µm, V_{ag}: 50, 100, 150, 200, 250, and 300 rpm; T : 20 °C; pH: 4.2; C_0: 60 mg/L, ms: 1 g, ΔV_{ag}: ±2 rpm
Impact of T	t_c: 50 min (alone), tc: 70 min (mixture), Øs: 200 µm, V_{ag}: 200 rpm; T: 20, 35, 45, and 55 °C; pH: 6; C_0: 60 mg/L, ms: 1 g, ΔT: ±0.8 °C
Impact of pH	t_c: 50 min (alone) ; t_c: 70 min (mixture); Øs: 200 µm, V_{ag}: 200 rpm; T: 20°C; pH: 2, 2.5, 3, 3.8, 4.2, 4.8 , 5.4, and 6; C_0: 60 mg/L, ms: 1 g, ΔpH: ±0.02
Impact of C_0	t_c: 50 min (alone), tc: 70 min (mixture), Øs: 200 µm,V_{ag} : 200 rpm; T: 20°C; pH: 6; $Ø_s$: 200 µm, C_0: 30-300 mg/L, ms: 1 g, ΔC_0: ±2 mg/L

3. Results and discussion

3.1 Characterization of adsorbent

XRF and XRD analyses were performed on the solid samples, specifically SS and SG. Table 3 presents the mass percentages of these materials, and Figures 1a and 1b provide an illustration of the XRD characterization for SS and SG, respectively. The latest results obtained from XRF analysis of SS slag have just reaffirmed the data reported in the literature [4,5], indicating that the major components of SS include lime (CaO: 35.2), silica (SiO_2: 40.85), alumina (Al_2O_3: 11.38), and magnesium oxide (MgO: 5.03) (Table 3).On the other hand, the analyses carried out on SG indicated a dominance of silica (SiO_2: 95.61%) (Table 3).

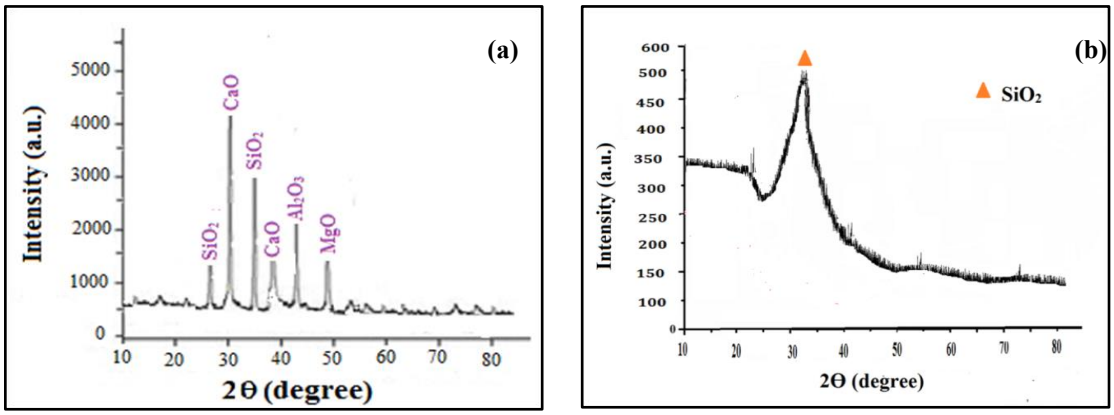

Figure 1: XRD spectrum: (a) Treated blast furnace slag [6], (b) Silica gel

Figure 1a demonstrates good agreement between the XRF and XRD analysis results. Effectively, high levels of lime and silica were identified, while alumina and magnesium oxide levels were lower. According to the SG analysis performed by XRD, a significant increase in the silica concentration was observed, with no traces of lime, alumina and sodium oxide (Figure 1b), suggesting a dispersion of these elements in the new structure.

The results of EDS analyses highlighted significant concentrations of silicon (Si), calcium (Ca), and oxygen (O), as well as lower levels of aluminum (Al) and magnesium (Mg), confirming that the SS is mainly composed of CaO, SiO_2, Al_2O_3, and MgO, present in different amounts (Figure 2a). From the observations made in Figure 2b, we found that SG is mainly

composed of silicon (Si) and oxygen (O). These findings indicate that SG consists primarily of silica (SO_2).

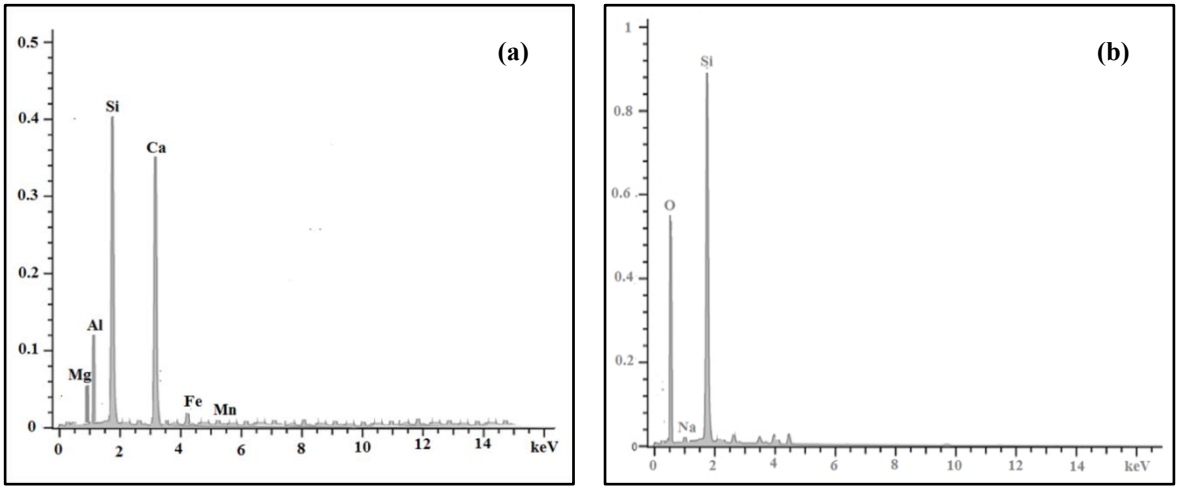

Figure 2: EDX spectrum: (a) Treated blast furnace slag, (b) Silica gel

Surface analyses of SG revealed that nitrogen adsorption and desorption follow a type IV isotherm (Figure 3a), indicating that SG exhibits a mesoporous structure characterized by H3-type hysteresis loops. This type of isotherm was related to the capillary condensation occurring within the mesoporous structure. The specific surface area obtained was 472.38 m²/g. The pore radius obtained was 10.98 nm (Figure 3b). The mesoporous configuration of SG certainly appears to play a role in the intensification of surface area and pore volume.

Table 3: Chemical composition of treated blast furnace slag [2,6], and silica gel (SG)

Element	**Mass (%)**		
	Treated slag	Silica gel	Error
CaO	35.21	0.87	±0.332
Al_2O_3	11.38	0.54	± 1.36
SiO_2	40.85	95.61	± 2.315
Fe_2O_3	1.36	0	±0.3327
MgO	5.03	0	±0.066
MnO	1.04	0	±0.143
K_2O	0.2	0	±0.0181
Na_2O	0.99	0.71	±0.141
P_2O_5	0	0.33	
LOI	3.94	1.94	±0.231

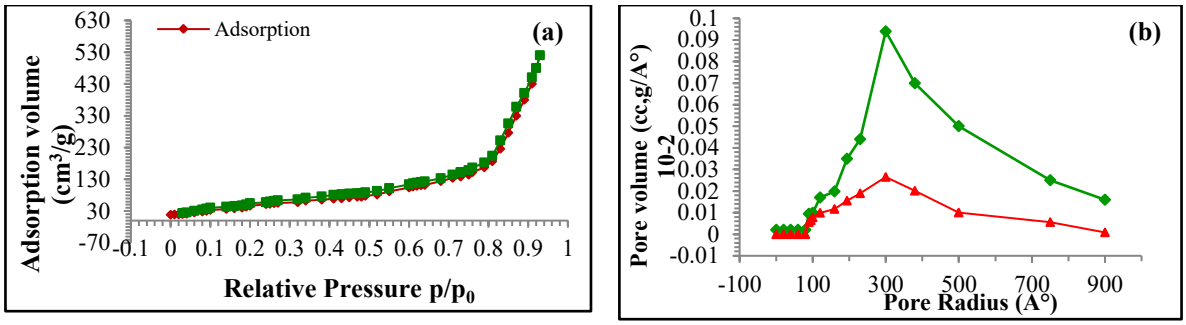

Figure 3: (a) N_2 adsorption-desorption isotherm of SG, (b) SG pore size and volume curve

3.2 Execution of the adsorption process

The adsorption of lead, nickel, and cadmium on SG in batch mode was accomplished by analyzing several successive factors, such as the contact time effect, the impact of agitation, the influence of the pH of the solution, the importance of the temperature, and the action of the initial concentration of the polluting solution. The experimental modalities implemented are presented in Table 1.

3.2.1 Contact time effect

The evolution of the adsorption process of the pollutants examined on SG as a function of the contact time was verified over a period ranging from 0 to 300 minutes (Figure 4a). During these processes, we observed rapid adsorption occurring in the first 30 minutes, then less intense processes between 30 and 50 minutes, followed by stabilization from 50 minutes, where the adsorption capacity reached 43.11, 38.88, and 35.12 mg/g for lead, nickel, and cadmium, respectively. The efficiency of the adsorption process during the first 30 minutes is mainly explained by the presence of numerous active adsorption sites, thus promoting strong interactions between the ions of the pollutants studied and the SG [8]. The reduced rate observed in the second stage primarily results from the gradual depletion of available adsorption sites [2]. The cessation of adsorption processes after 50 minutes results from the filling of active sites on the adsorbent surface, which indicates saturation of the SG [9,29].

Examination of the evolution of the adsorption of the Pb-Ni-Cd mixture on SG according to the contact time, ranging from 0 to 300 minutes (Figure 4b), showed a continuous and quasi-homogeneous adsorption during the period from 0 to 70 minutes, which corresponds to the saturation time. For the mixture (Pb-Ni-Cd), the adsorption capacity is 28.45 mg/g, while the individual capacities of lead, nickel, and cadmium are 12.19, 9.46, and 6.8 mg/g, respectively. The difference in equilibrium time between the adsorption of the mixture and that of monoadsorption is mainly caused by the competition between the metal ions involved [8,10]. Indeed, the competition between the metal ions generates partial barriers that slow down the logical transfer process. From these results, we estimated that the saturation of the SG absorbing surface for the separate adsorption of lead, nickel, and cadmium is 50 minutes and 70 minutes for the tertiary mixture (Pb-Ni-Cd).

3.2.2 Influence of particles size

The particle size of the adsorbent plays a key role in the transfer of metal ions from the solution to the adsorbent [2]. In this context, we adjusted the particle size of SG by choosing diameters ranging from 50 to 400 µm, as shown in Figure 3c. According to the results obtained, the efficiency of ion adsorption on SG is maximum for particles of size 200 µm. Indeed, the adsorption capacities were observed to decrease, reaching 8.23 mg/g for lead, 7.84 mg/g for nickel, 6.34 mg/g for cadmium, and 5.83 mg/g for the mixture, these values corresponding to particle sizes varying between 400 and 200 µm. The reduction in particle size resulted in an

increase in the adsorption surface of the SG, which led to an increase in the adsorption rate [32]. For particles with a diameter of less than 200 µm, the adsorption of pollutants analyzed by the SG is the least favorable. This result is perhaps due to the emergence of the coalescence phenomenon. That is, a return to large diameters [4].

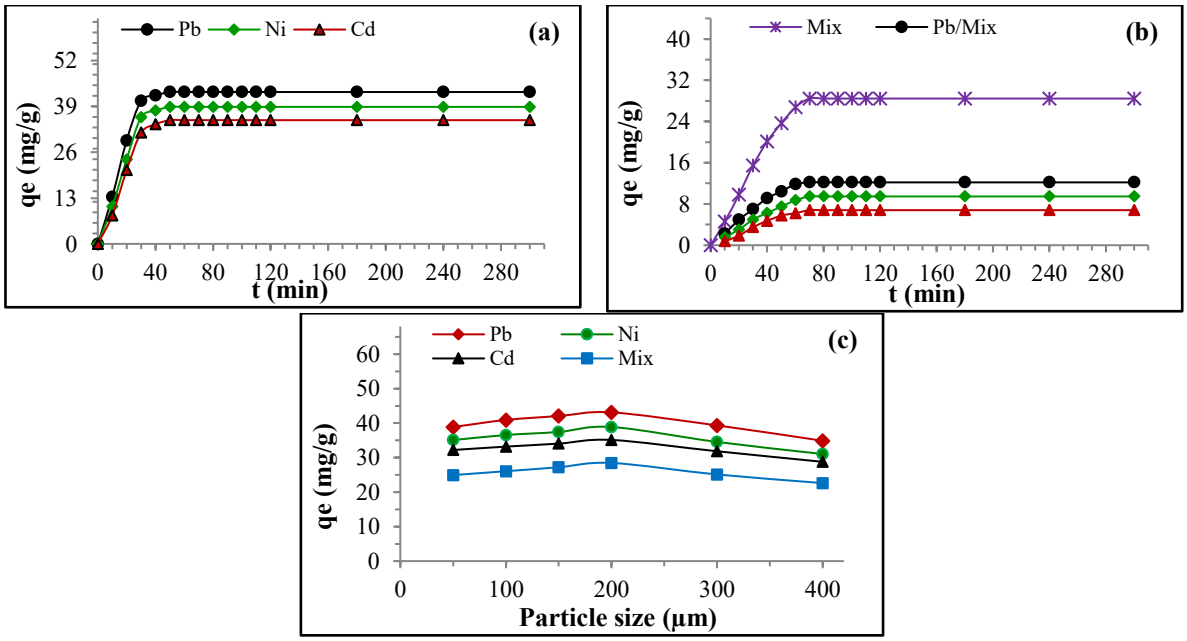

Figure 4: Effect of contact time: (a) adsorption of lead, nickel and cadmium alone, (b) adsorption of lead, nickel and cadmium in mixture, (c) Influence of particles size

3.2.3 Agitation speed effect

Agitation of the medium is a critical factor, significantly enhancing the transfer of pollutants from the solution to the solid-liquid interface via external diffusion [2,4]. Accordingly, the system was stirred the medium from 50 to 300 rpm (Figure 5a). According to the observations in Figure 5a, the adsorption efficiency evolved gradually with speeds ranging from 50 to 200 rpm, showing an increase in the adsorbed amount of 12.13, 11.21, 11.58, and 10.65 mg/g, respectively, for the adsorption of lead, nickel, cadmium, and the ternary mixture. The efficient distribution of SG particles throughout the contaminated solution, accompanied by an increase in the diffusion coefficient, was fundamental to ensuring the adsorption efficiency of the pollutants examined [5,10]. Beyond 200 rpm, we observed that the elimination of the pollutants studied stabilized, without variations in the adsorption capacity values. The stability of the process probably resulted from the cessation of the external transfer of the metal ions examined from the solution to the adsorbent surface of the SG [2,5]. These data demonstrate that 200 rpm provides the ideal agitation for effective adsorption.

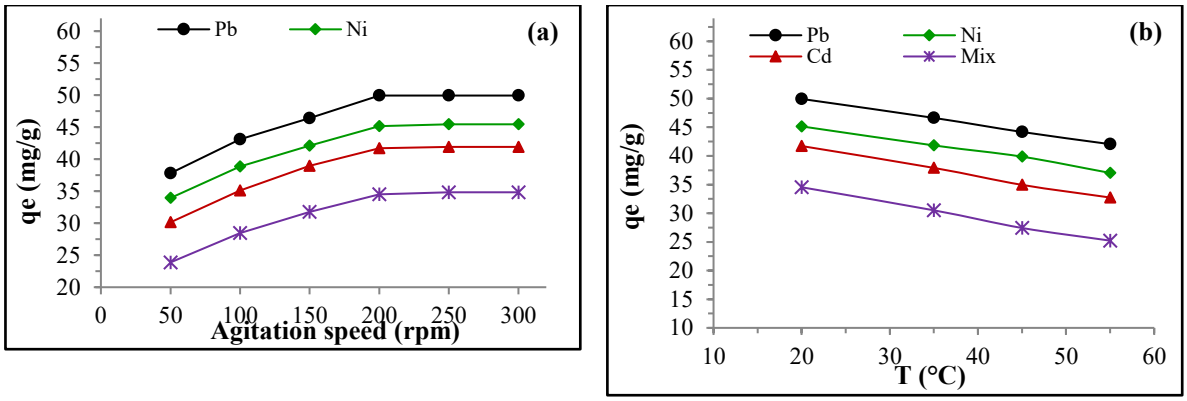

Figure 5: Plots: (a) Effect of agitation speed, (b) Effect of temperature

3.2.4 Effect of temperature

The effect of different medium temperatures, including 25, 35, 45, and 55°C, was examined in the adsorption processes of lead, nickel, cadmium, and the ternary mixture in aqueous medium by SG (Figure 5b). The research conducted showed that the abilities to remove the discussed pollutants would decrease with the increase of the solution temperature. In fact, it was specified that the adsorbed quantity measured between 20 and 55°C decreased by 7.89, 8.12, 8.98, and 9.31 mg/g for adsorption lead, nickel, cadmium, and mixture, respectively. The increase in temperature may have weakened the action of electrostatic interaction with active adsorption sites, thus leading to the involution of the adsorption process [2,30]. Based on this investigation, it can be inferred that the adsorption of lead, nickel, cadmium, and the ternary mixture on SG in solution is likely an exothermic process [29,31].

3.2.5 Effect of pH

It is well established in adsorption techniques that the pH of the solution has a determining influence in achieving a significant adsorption capacity [1,4]. With this in mind, we varied the pH between 2 and 6 (Figure 6b). We are limited to a pH of 6 so as not to disturb the adsorption processes examined, because lead, nickel and cadmium hydroxides are formed above pH 6 [9,14]. From Figure 6a, we observed that the curves cross the X-axis at 3.4 on the pH scale, indicating that the PZC is 3.4. According to Figure 6b, it was noticed that at a pH higher than 3.8, a good correlation is manifested between the adsorption of the pollutants analyzed and the properties of the media used. Indeed, the adsorption performances improved considerably during this interval. This effect appears to be caused by the nature of the charge established on the adsorbent surface (negative charge); moreover, it is caused by the progressive decrease of H^+ ions, which will strengthen the electrostatic interaction between the analyzed metal ions, namely Pb(II), Ni(II), Cd(II), and Pb-Ni-Cd, as well as the active adsorption sites of SG [3]. Under pH ≤ 3 conditions, limited adsorption was observed; the adsorption rates did not exceed 11.8% (Pb(II)), 10.05% (Ni(II)), 7.86% (Cd(II)), and 5.76% (Pb-Ni-Cd). The process impairment is mainly inflicted by an excess of protons that restricts the movement of pollutants from solution to the SG adsorbent surface [2,5]. In addition, the absorbent surface has a lower pH than the PZC, which makes it positively charged and generates a repulsion phenomenon [6].

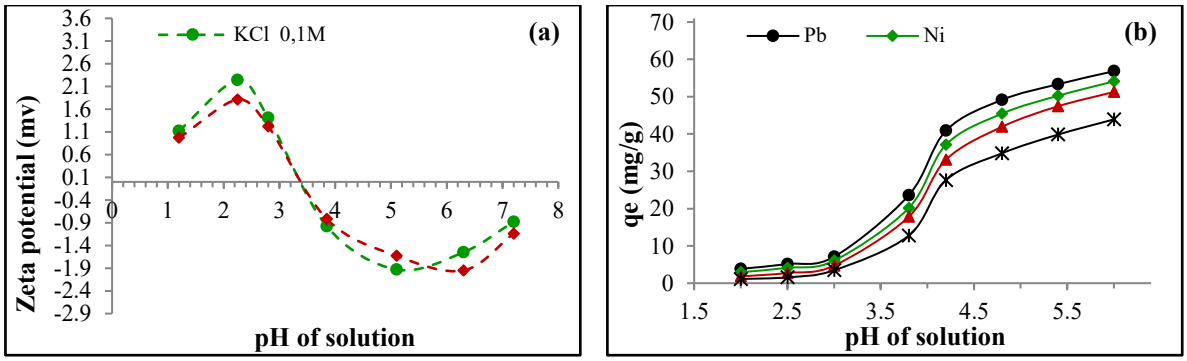

Figure 6. Plots of (a)Zero-charge point analysis, (b) Effect ofinitial pH

3.2.6 Effect of Initial Concentration

To represent the experimental adsorption isotherm and evaluate the maximum adsorption amount, we investigated the influence of the initial concentration on the adsorption processes of lead, nickel, and cadmium individually (Figure 7a), as well as on a tertiary mixture containing these three elements at equivalent concentrations (Figure 7b). According to Figure 7a, the adsorption capacity was shown to vary in two main phases. First, the adsorption extent increased in response to the increase in the initial concentration, where we observed that at C_0 = 240 mg/L the adsorption capacities had reached a maximum level, namely 144.74, 133.14, 126.86, and 119.12 mg/g for lead, nickel, cadmium and the tertiary mixture, respectively. The enhancement of adsorption capacity was probably caused by the establishment of a strong driving force generated by the intensive supply of metal ions in solution, thereby decreasing the opposition to mass transfer and stimulating the diffusion of studied pollutants from solution to the SG adsorbent surface [2,4]. In phase two, the observed adsorption processes did not show any reaction, even with the increase in the initial concentration of the metal pollutants concerned, and the adsorption capacities remained constant. This means that the active surface is saturated, which explains the inactivity of the processes studied [10].It is most likely that the partial decrease in the adsorbed amount of the ternary mixture compared to the separate elements is caused by the rivalry between the lead, nickel, and cadmium ions in contact with the solid-liquid interface [3,8,10]. The observed adsorption values for lead, nickel and cadmium in the mixture were 48.18 mg/g, 40.22 mg/g and 30.72 mg/g, respectively, indicating that SG displays a higher affinity for lead, followed by a reduced affinity for nickel and finally for cadmium. This makes perfect sense, since lead has the lowest hydrated ionic radius (4.01 Å), followed by nickel (4.04 Å) and finally cadmium (4.26 Å) [8,32]. The electronegativity indices of lead (2.33), nickel (1.91), and cadmium (1.69) also support our deduction. From the results obtained, we noted a decrease in the adsorption percentage of the pollutants examined due to the increase in concentration (Figure 7b). This is considered very consistent, since the active surface of the SG gradually saturates as the initial concentration increases and becomes inaccessible from a certain threshold, and therefore the removal percentage constantly decreases [9].

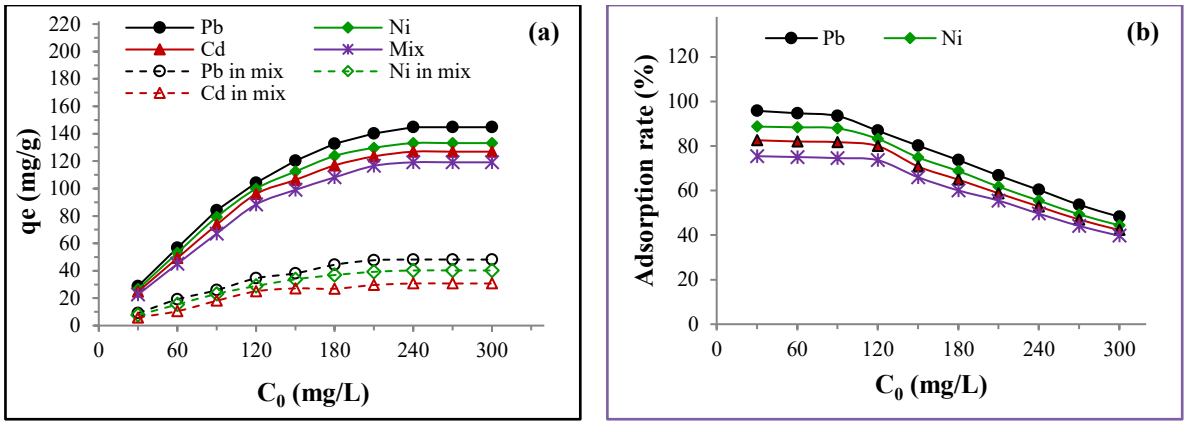

Figure 7: Effect of initial concentration (a) Adsorption capacity, (b) Adsorption rate

Similar research on the adsorption of lead, nickel, cadmium alone and in ternary mixtures has been reported in the literature, particularly concerning the application ofcocoa pod husks [3], porous geopolymer foams [8], modified sulfonated graphene oxide composite [9], macroporous γ-alumina [33], and mesoporous and nanomesoporous silica [34].These studies revealed that all adsorbents used were highly attractive to lead but exhibited distinct affinities for nickel and cadmium ions.

3.3 Adsorption isotherms

The dispersion of pollutants between the liquid phase and the solid phase can be interpreted through adsorption isotherm models. Effectively, the adsorption isotherm is crucial to understanding the reaction dynamics between the adsorbate and the adsorbent. Furthermore, the results demonstrate both the surface properties and adsorption affinity of the material. In this study, we chose to use the Freundlich, Langmuir, and Temkin adsorption isotherm models in order to more precisely evaluate the maximum adsorption quantities and to explore in depth the relationships that occur during these processes.

It is worth noting that the Freundlich model has been used to symbolize the adsorption process on heterogeneous surfaces in a reversible system [10]. Its linear form can be represented by equation 4.

$$\log q_e = \log k_1 + \frac{1}{n}\log C_e \quad (4)$$

Where q_e= experimental maximum quantity (mg/g), C_e= equilibrium solution concentration (mg/L), k_1= Freundlich constant (mg/g)(mL/mg)$^{1/n}$, and $1/n$ = heterogeneity factor.

On the other hand, the Langmuir model has been used to model the adsorption process on a homogeneous monolayer surface, where each adsorption site can accommodate only one molecule [14]. Its linear form can be presented by equation 5. One of the important aspects of the Langmuir model is the separation factor (R_L). This dimensionless factor can help specify the nature of the adsorption process. Indeed, we consider that adsorption is favorable when the coefficient R_L is between 0 and 1; it is called linear when R_L is equal to 1, and it becomes irreversible if R_L is equal to 0 [2]. The R_L can be determined from equation 6.

$$\frac{C_e}{q_e} = \frac{1}{q_{max}} C_e + \frac{1}{q_{max} k_2} \quad (5)$$

$$R_L = \frac{1}{1+C_0 k_2} \quad (6)$$

Where q_{max}= theoretical maximum quantity (mg/g), q_e= experimental maximum quantity (mg/g), C_0 = concentration of the initial solution (mg/L), C_e = equilibrium solution concentration (mg/L), and k_2= Langmuir constant (L/mg).

While the Temkin adsorption isotherm is based on the assumption that the heat of adsorption of each molecule in a layer decreases linearly with the degree of coverage due to the interactions between the adsorbed molecules and the adsorbent and that the adsorption has a homogeneous distribution of binding energies up to a maximum binding energy [6]. Its linear form can be presented by Equation 7.

$$qe = B_T \ln A_T + B_T \ln Ce \quad (7)$$

Where, $B_T = \frac{RT}{b_T}$, A_T= equilibrium binding constant (L/g), R= universal gas constant (8.314 J/mol/K), T= temperature at 298K, and b_T= constant related to heat of sorption (kJ $kmol^{-1}$)..

Figures 8(a), 8(b), 8(c), and 8(d) show the adsorption isotherm curves of lead, nickel, cadmium, and the mixture (Pb-Ni-Cd), respectively. Table 3 lists the parameters related to the discussed models. The plots of the Freundlich, Langmuir, and Temkin models for the adsorption of lead, nickel, cadmium, the mixture, lead in the mix, nickel in the mix, and cadmium in the mix are shown in Figures 1S, 2S, 3S, 4S, 5S, 6S, 7S, respectively (supplementary file). The evolution of the separation factor R_L is represented in Figure 9.

Following the analysis of experimental data through modeling, it was observed that the values of the correlation coefficient (R^2) obtained by the Langmuir model for the adsorption of lead, nickel, and cadmium were 0.999, 0.998, and 0.999, respectively. On the other hand, the values were 0.882, 0.875, and 0.853, respectively for the Freundlich model, while they were 0.956, 0.952, and 0.945 for the Temkin model. In addition to this result, it was observed that the maximum capacities, theoretically derived from the Langmuir model, aligned almost perfectly with the measured adsorption values, as presents in Table 4. The same conclusions were drawn regarding the adsorption of lead, nickel and cadmium in a ternary mixture, the correlation coefficients of the Langmuir model being higher than those of the Freundlich and Temkin, models; see Table 4. As a result of this outcome, it was estimated that the adsorption of lead, nickel and cadmium, whether alone or in a mixture, was carried out on a homogeneous monolayer surface [2,20].

Table 4: Characteristics of the analyzed isothermal models

Model	Parameter	Pb(II)	Ni(II)	Cd(II)	Mix	Pb(II) in mix	Ni(II) in mix	Cd(II) in mix
Freundlich	K_1 $(mg.g^{-1})(ml.mg^{-1})^{1/n}$	37.78	28.90	21.75	13.74	15.27	7.48	3.70
	1/n	0.301	0.337	0.382	0.459	0.339	0.468	0.553
	R^2	0.882	0.875	0.853	0.843	0.822	0.861	0.827
Langmuir	q_{max} (mg/g)	144.92	134.95	125.95	120.19	44.92	41.66	33.11
	K_2 $(L.mg^{-1})$	0.181	0.21	0.082	0.048	0.34	0.13	0.07
	R^2	0.999	0.998	0.999	0.991	0.996	0.990	0.941
Temkin	b_T (kJ/mol)	0.116	0.111	0.099	0.091	0.269	0.236	0.201
	A_T (L/g)	4.16	1.86	1.15	2.91	3.94	1.14	1.93
	R^2	0.956	0.952	0.945	0.941	0.931	0.952	0.943

Based on Figures 8(a), 8(b), 8(c), and 8(d), it was observed that the adsorption isotherms according to the Langmuir model more faithfully reflect the experimental results. Their evolution is gradual until the adsorbent surface of SG is saturated, after which their behaviors become constant, generating a straight line [2,6]. In parallel, the Freundlich and Temkin

isotherms show a different progression, with maximum capacities much higher than the experimental values observed. From these analyses, we were also able to confirm that the adsorption of the pollutants studied on SG follows the Langmuir model.

From Figure 9, it was observed that the separation coefficient R_L for the adsorption of elements, whether present individually or in mixture, decreased with the increase in the initial concentration, over a range between 0 and 1. Indeed, for lead, the R_L decreased from 0.155 to 0.018, while for nickel, it decreased from 0.215 to 0.026. Concerning cadmium, it decreased from 0.28 to 0.038. As for the mixture, the R_L decreased from 0.22 to 0.028 during the adsorption of lead, while it decreased from 0.434 to 0.071 during the adsorption of nickel, and finally, it dropped from 0.555 to 0.111 during the adsorption of cadmium. These results indicate favorable adsorption for all processes accomplished [2,8].

The nature of the adsorption processes can also be characterized by the value of the heterogeneity factor (1/n), one of the parameters of the Freundlich model. Indeed, the adsorption can be described as linear when 1/n = 1; it is assumed to be chemical when 1/n > 1, and it is considered physical and favorable when 0 < 1/n < 1 [20,35]. In this work, the calculated heterogeneity value (1/n) is 0.301 for lead, 0.337 for nickel, 0.382 for cadmium, and 0.459 for the ternary mixture (Table 4), thus indicating that the removal of the elements examined is favorable and was accomplished by physical adsorption [35].

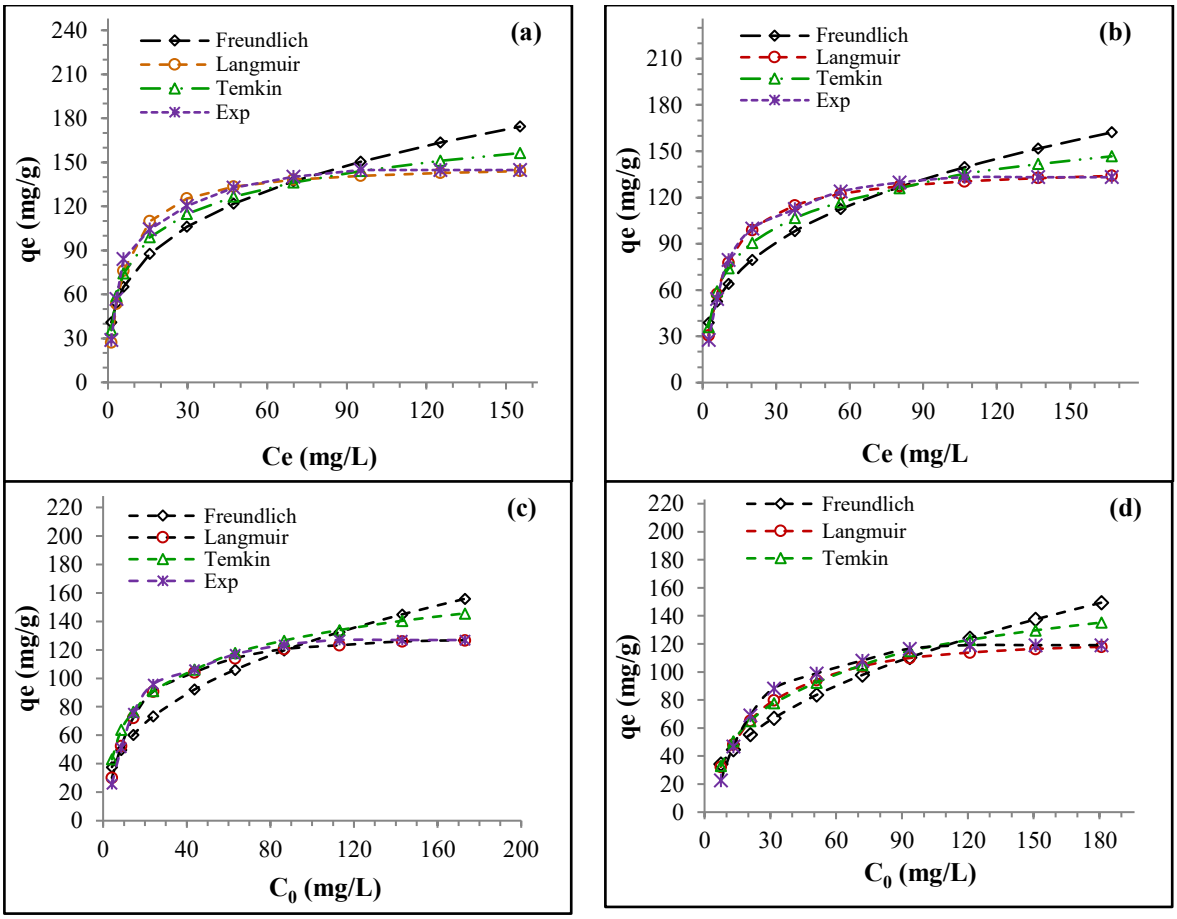

Figure 8: Adsorption isotherms (a) Lead, (b) Nickel, (c) Cadmium, (d) Ternary mixture

From Table 4, it was also noted that the b_T value is less than 8 kJ/mol, which also confirms that the removal of lead, nickel, cadmium, and the ternary mixture by SG was achieved by physical adsorption under the effect of electrostatic interactions [36]. Furthermore, Table 4 shows that

the highest K_2 value was obtained for lead, followed by nickel and cadmium, indicating that GS exhibits the strongest adsorption affinity for Pb, both in single-component and mixed systems [9,33].

This study leads us to conclude that the ions of the pollutants analyzed adsorb on a uniform monolayer surface thanks to slight physical interactions, such as those of van der Waals, which indicates that the methods implemented are associated with relatively low adsorption energies [35,37].

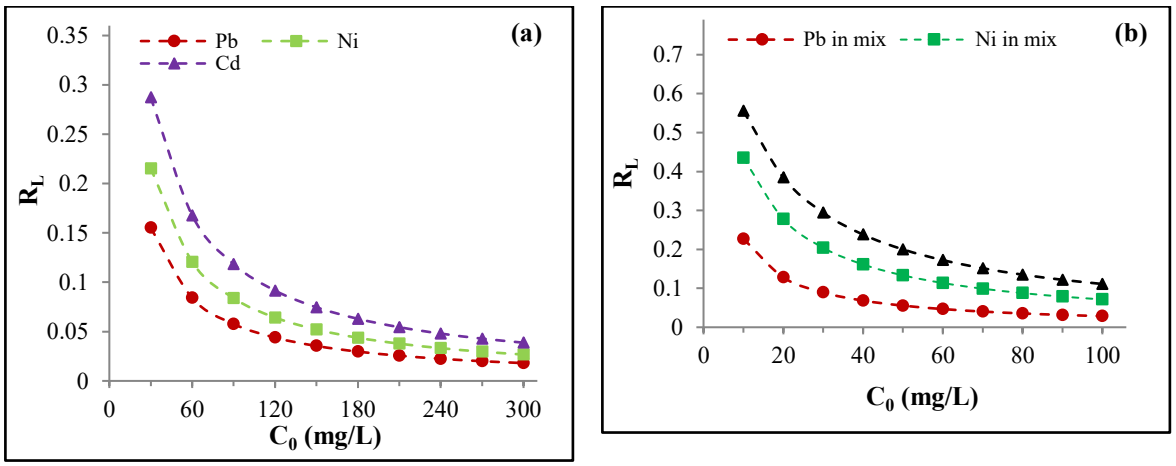

Figure 9: Evolution of the separation factor R_L: (a) adsorption of elements alone, (b) adsorption of the mixture

3.4 Adsorption kinetics

In order to thoroughly analyze the adsorption mechanisms of lead, nickel, and cadmium, both individually and in tertiary mixtures, we used mathematical models adapted to the adsorption processes. These include pseudo-first-order (PFO), pseudo-second-order (PSO), external diffusion (ED), and intraparticle diffusion (IPD) models.

$$\log(q_e - q) = -k_3 t + \log q_e \quad (8)$$

$$\frac{t}{q} = \frac{1}{k_4 q_e^2} + \frac{t}{q_e} \quad (9)$$

$$q = k_5 \sqrt{t} + C_{In} \quad (10)$$

$$\log C_e = k_6 t + C_{Ex} \quad (11)$$

Where C_e= equilibrium concentration (mg/L), qe experimental adsorption capacity (mg/g), q= calculated adsorption capacity at time t (mg/g), k_3: pseudo-first-order constant (min^{-1}), k_4= pseudo second order constant (g/mg min), k_5= internal diffusion constant (mg/m. min ½), k_6= external diffusion constant (min^{-1}), C_{In} = interception of internal diffusion and C_{Ex} = interception of external diffusion.

The adsorption kinetics of lead, nickel, cadmium, and ternary mixture according to PFO and PSO models are shown in Figures 10a and 10b, respectively, while the analysis of external and intraparticle diffusion is symbolized in Figures 11a and 11b separately. The parameters of the pseudo-order models are reported in Table 5, while the diffusion models are collected in Table 6.

From the results obtained, it was shown that the correlation coefficients of the PSO model ($0.991 \leq R^2 \leq 0.999$) for all the analyzed processes were higher than those of the PFO model ($0.889 \leq R^2 \leq 0.95$). In addition, the values of the adsorption capacities according to the PSO

model were almost similar to those offered by the experimental tests (Table 5). Based on this information, we could conclude that the adsorption processes of lead, nickel, cadmium, and the ternary mixture follow pseudo-second-order kinetics [20,27,34]. Similar examples of the adsorption of lead, nickel, cadmium, and ternary mixture have been reported in the literature with other materials, including cocoa pod husks, modified sulfonated graphene oxide composite, macroporous γ-alumina, polymer nanocomposites, and mesoporous and nanomesoporous silica [3,9,33,36].

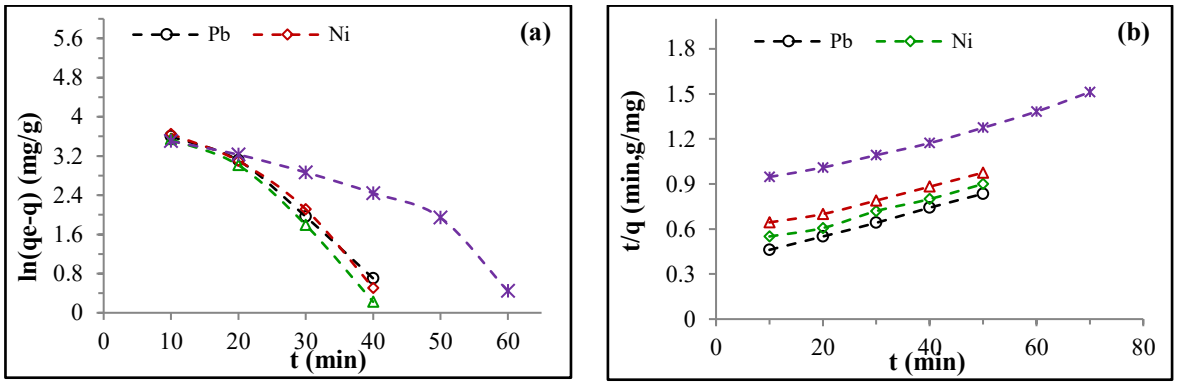

Figure 10: Adsorption kinetics of the studied metal ions: (a) According to the PFO model, (b) According to the PSO model

Analysis of Figure 11a plotted from the IPD model revealed that the lines did not cross the origin ($C > 0$) and exhibited various linear behaviors for all adsorption processes studied. These observations allowed us to deduce that intraparticle diffusion (IPD) is not the only mechanism controlling the adsorption processes of lead, nickel and cadmium alone or in the mixture [3]. The observed multiple linearity refers to the presence of multiple mechanisms controlling the processes conducted [4,35], where each line fraction can embody one or more control regimes. Indeed, the first segments describe the transfer of lead, nickel, and cadmium ions from the solution to the boundary layer via an external diffusion mechanism, while the second segments emphasize the progressive movement of these ions from the active surface of the SG to the internal pores by intraparticle diffusion. After a certain duration (equilibrium time), the studied processes reach a steady state and stop when the active adsorption sites are completely filled. It is important to note that the removal of lead, nickel, and cadmium, whether individually or in mixture, occurs more slowly as the adsorbent surface approaches saturation, which reduces the efficiency of intraparticle diffusion [35]. It was noticed that the values of the rate constant k_5 during the first phase are considerably higher than those obtained during the second phase, while the intercept values (C_{In}) show an opposite, trend; see Table 6.

These indices reaffirm that the processes examined are faster during the first phase, and long during the second phase. As a result of this analysis, we were able to see that the presentation derived from the IPD model is adaptable for the diffusion of metal ions from the liquid phase to the solid phase, both internally and externally.

From the presentations derived from Equation 11, it was noticed that the alignment of the set of points studied was formed by straight lines, where the correlation coefficient of each straight line exceeds 0.99, as demonstrated in Table 6 and Figure 11b. Based on this information, we can deduce that the transfer of lead, nickel, cadmium, and the mixture from the liquid phase to the solid phase is regulated by external diffusion as the first step [2,4,6]. From this part, we can affirm that the transport mechanism of the considered metal ions, passing from the liquid phase

(solute) to the solid phase (adsorbent), is largely controlled by external diffusion, followed by diffusion inside the particles [6,29,35].

Table 5: Kinetic parameters of pseudo-order models

Element	PFO				PSO			
	qe_{exp} (mg/g)	q_{theo} (mg/g)	K_1 (min^{-1})	R^2	qe_{exp} (mg/g)	q_{theo} (mg/g)	K_2 (g/mg min)	R^2
Pb(II)	56.83	74.449	0.098	0.937	56.83	57.47	0.0174	0.999
Ni(II)	54.11	78.25	0.01	0.928	54.11	53.19	0.0188	0.992
Cd(II)	51.26	79.83	0.011	0.931	51.26	51.26	0.0198	0.992
Mixture	46.91	80.72	0.055	0.889	46.91	46.91	0.0209	0.991

Table 6: Kinetic parameters of diffusion models

Element	ED			IPD					
				1st linear part			2nd linear part		
	C_{Ex}	K_5 (min^{-1})	R^2	C_{In}	K_5 (mg/g.min)	R^2	C_{In}	K_5 (mg/g.min)	R^2
Pb(II)	4.31	0.093	0.996	10.82	17.62	0.999	38.91	2.49	0.999
Ni(II)	4.24	0.074	0.992	13.24	14.94	0.998	32.48	2.29	0.972
Cd(II)	4.15	0.051	0.991	14.82	13.66	0.994	31.90	2.03	0.988
Mixture	4.12	0.021	0.999	11.79	12.41	0.998	21.13	3.81	0.984

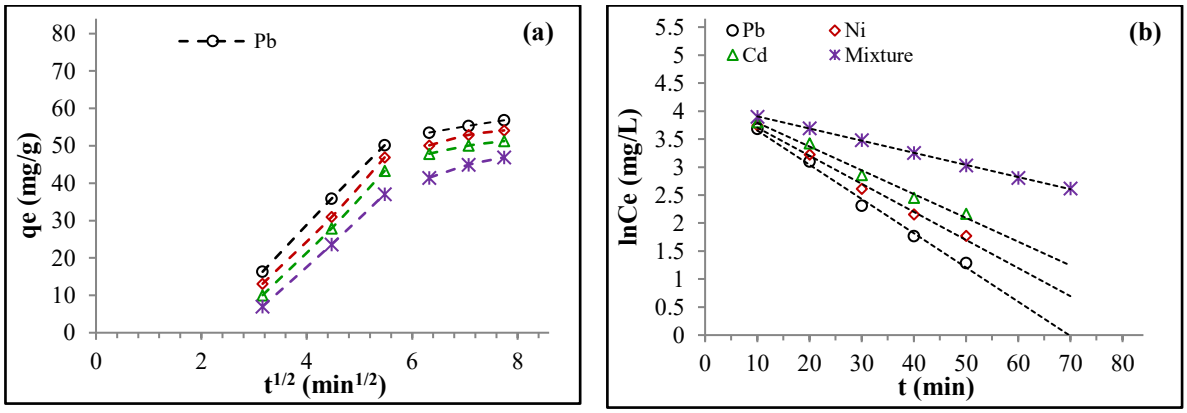

Figure 11: diffusion kinetics of the studied metal ions: (a) According to the IPD model, (b) According to the ED model

3.5 Thermodynamic study

In this section, a thermodynamic analysis was carried out to elucidate the nature and interaction mechanisms affecting the removal of lead, nickel, cadmium and their ternary mixtures. These effects are mainly explained by the values of Gibbs energy (ΔG°), enthalpy (ΔH°), and entropy (ΔS°). ΔG°, ΔH°, and ΔS° were evaluated using equations 12 and 13 [16]. The distribution coefficient k_d was determined from equation 14. The mechanism promoting lead adsorption was verified by the value of the activation energy as defined in equation 13 [38].

$$\Delta G^0 = -RT\ln k_d \quad (12)$$

$$\ln k_d = \frac{\Delta H^0}{R} \times \frac{1}{T} + \frac{\Delta S^0}{R} \quad (13)$$

$$k_d = \frac{C_i - C_e}{C_e} \times \frac{V}{M} = \frac{q_e}{C_e} \quad (14)$$

Where ΔG°= Gibbs free energy (kJ/mol), ΔS°= entropy (J/molK), ΔH°= enthalpy (J/mol), R= the universal gas constant (8.314 J/molK), k_d= distribution coefficient (L/g), and T= absolute temperature (K).

Data on thermodynamic parameters and distribution coefficient are shown in Table 7. The plot of Van't Hoff's equation (Eq.13) is represented by Figure 12.

From Figure 12 and Table 7, it was observed that there was an excellent correlation between the results of the Van't Hoff model and the experimental data relating to the adsorption of the pollutants studied ($R^2 > 0.990$), which demonstrates that the processes carried out are favorable [8].The reduction in K_d recorded with increasing temperature highlighted that the techniques used lose effectiveness in aqueous media at higher temperatures [7].The negative values of the thermodynamic parameters, namely ΔG°, ΔH°, and ΔS° (Table 7), prove that the four adsorption processes performed are spontaneous, exothermic, and exhibit low entropy [22,27,29,38].

The reduction of the ΔG° value with increasing solution temperature revealed that the mass transfer of metal ions from the solution to the SG adsorbent surface was reduced with increasing medium temperature due to the reduction of the driving force [7]. Since the ΔG values for all the analyzed processes range from -20 to 0 kJ/mol (see Table 7), we conclude that these processes were carried out by physical adsorption under the influence of electrostatic interactions [6,35]. From Table 7, it appears that the enthalpy value (ΔH°) for the adsorption of lead (-8.22 kJ/mol), nickel (-7.18 kJ/mol), cadmium (-6.59 kJ/mol), and the ternary mixture (-5.92 kJ/mol) is less than 40 kJ/mol, which indicates that the adsorption of the mentioned elements was carried out by a physical adsorption process [2,35,38,39]. The negative values of the calculated entropies revealed that the random motion at the interface of SG and metal ions has decreased (Table 7) [2,4]. This demonstrates that the distribution order of the studied metal pollutants on the adsorbent surface of SG has evolved compared to that of the solution [15]. The decrease in random motion was probably caused by the electrostatic interactions existing between the adsorbate and the adsorbent [22,36]. From these results, it was clarified that the adsorption of lead, nickel, cadmium, and the ternary mixture by SG is better represented by the Langmuir model due to the regular arrangement of these metals on the active adsorption sites [37].

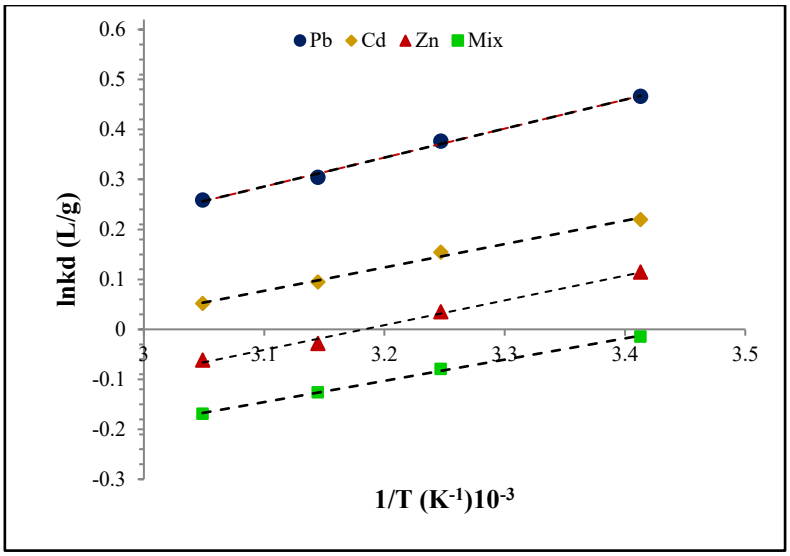

Figure 12: Van't Hoff's plot

Table 7: Thermodynamic parameters of adsorption processes executed

Element	T (K)	ΔH° (kJ/mol)	ΔG° (kJ/mol)	ΔS° (J/mol.K)	K_d (L/g)	R^2
Pb(II)	293	-8.228	-17.975	-12.579	1.593	0.996
	308		-18.666		1.457	
	318		-19.080		1.355	
	328		-19.557		1.295	
Ni(II)	293	-7.185	-17.375	-13.120	1.245	0.993
	308		-18.096		1.166	
	318		-18.526		1.099	
	328		-18.992		1.053	
Cd(II)	293	-6.597	-17.118	-11.423	1.121	0.994
	308		-17.791		1.035	
	318		-18.201		0.972	
	328		-18.683		0.940	
Mixture	293	-5.923	-16.803	-12.172	0.985	0.998
	308		-17.498		0.923	
	318		17.941		0.881	
	328		-18.389		0.844	

The removal of metal ions, whether individually or as a ternary mixture, occurs primarily through physical adsorption due to electrostatic interactions on a homogeneous surface of monolayer type. Accordingly, the proposed mechanisms are illustrated in Figure 13.

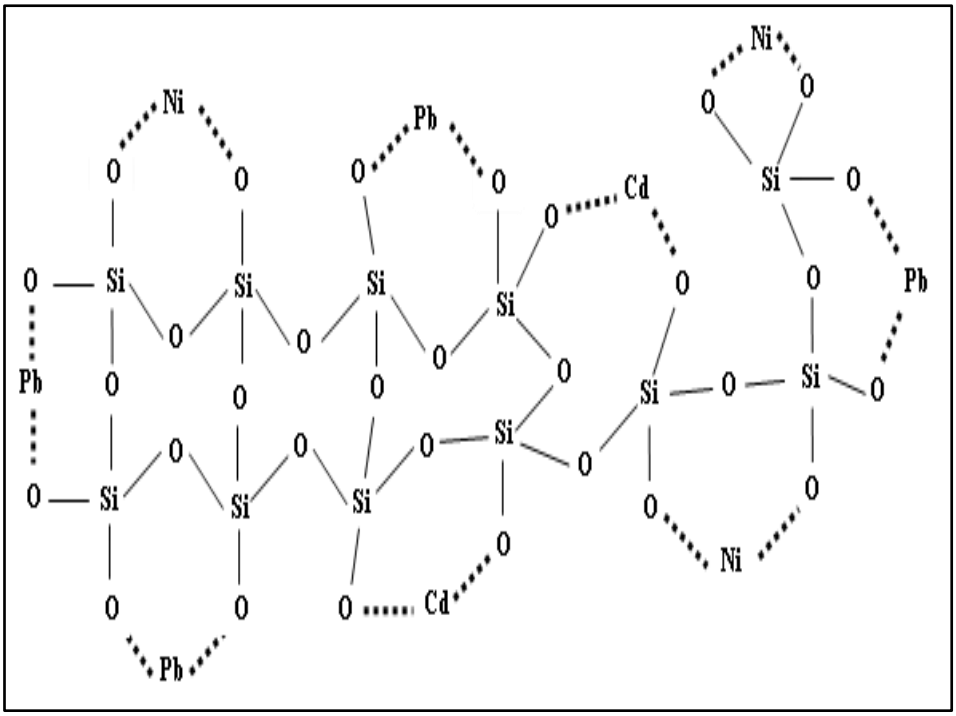

Figure 13: Adsorption mechanism ternary mixture

Conclusion

This study evaluated the effectiveness of a silica-based material (SG) synthesized from sslag (SS) for remove lead, nickel, and cadmium, both separately and in a ternary, through a batch mode adsorption process. Comprehensive experimental results revealed that the SG consists of 95.61% silica (SiO_2), with a zero charge point of 3.4 on the pH scale and a large specific surface area of 472.38 m^2/g. The experiments revealed that the saturation of the active surface of SG under the influence of stirring speed (200 rpm), solution pH (6), temperature (20°C), and initial concentration (240 mg/l) was identified after 50 minutes of contact, where the adsorption amounts of lead, nickel, and cadmium reached their highest levels, namely 144.74, 133.14, and 126.89 mg/g. For the adsorption of the ternary mixture, equilibrium was observed after 70 minutes of stirring under the influence of the same magnitudes of the determining factors. The adsorbed amounts of lead, nickel, and cadmium in the mixture were 48.18, 40.22, and 30.72 mg/g, respectively. The modeled experimental data demonstrated that the adsorption of metallic pollutants, separately and in mixture, was performed on a homogeneous monolayer surface. The separation factor (R_L) values demonstrated that the processes performed are favorable. The b_T values highlighted that the processes performed were carried out by physical adsorption. The heterogeneity factor (1/n) values revealed that the processes performed are favorable and were produced by physical adsorption. The kinetic study highlighted that the adsorption processes of lead, nickel, cadmium, and the mixture follow pseudo-second-order kinetics ($R^2 \geq 99$) and that the transport of metallic pollutants is controlled by external diffusion and intraparticle diffusion. The thermodynamic study reported that the adsorption of metallic pollutants individually or in ternary mixture is a spontaneous, exothermic, and low-entropic phenomenon. The values of Gibbs energy and enthalpy reaffirmed that the processes carried out were carried out by physical adsorption.

Conflict of interest

The authors declare that they have no known competing financial interests or personal relationships that could have appeared to influence the work reported in this paper.

References

[1] K.J. Abdallah and H.S. Abdulhay, "The adsorption of Cadmium and Lead Ions from aqueous solutions usingnon living biomass of Phragmites australis," *Iraqi Journal of Science*, vol. 58, pp: 427-434, 2017.

[2] T. Chouchane, S. Chibani, O. Khireddine and A. Boukari, "Adsorption study of Pb(II) ions on the blast furnace slag (BFS) from aqueous solution," *Iranian Journal of Materials Science and Engineering*, vol. 20, pp. 1-13, 2023, DOI:10.22068/ijmse.3011.

[3] C. Tejada-Tovar, A. Villabona-Ortíz and A. Gonz´alez-Delgado, "Adsorption study of continuous heavy metal ions (Pb^{2+}, Cd^{2+}, Ni^{2+}) removal using cocoa (Theobromacacao L) pod husks," *Materials*, vol. 15, no 6937, 2022. DOI:10.3390/ma15196937

[4] T. Chouchane, O. Khireddine and A. Boukari, "Kinetic studies of Ni(II) ions adsorption from aqueous solutions using the blast furnace slag (BF slag)," *Journal of Engineering and Applied Science*, vol. 68, no 34, 2021. DOI:10.1186/s44147-021-00039-3

[5] P. Djomgoue, M. Siewe, E. Djoufac, P. Kenfack and D. Njopwouo, "Surface modification of Cameroonian magnetite rich clay with Eriochrome Black T. Application for adsorption of nickel in aqueous solution," *Applied Surface Science*, vol. 258, pp. 7470-7479, 2012. DOI:10.1016/j.apsusc.2012.04.065

[6] T. Chouchane, M.T. Abedghars, S. Chouchane, H. Meradi and A. Boukari, "Use of Modified Blast Furnace Slag for Cadmium Removal in An Aqueous Medium," *Applied Environmental Research*, vol. 46(2), no 027, 2024. DOI:10.35762/AER.2024027.

[7] M. Hutton, "Sources of cadmium in the environment," *Ecotoxicology and Environmental Safety,* vol. 7, pp. 9-24, 1983. **DOI:10.1016/0147-6513(83)90044-1**

[8] Y. Liu, Y. Meng, X. Qiu, F. Zhou, H. Wang, S. Zhou and C. Yan, "Porous geopolymer foams for adsorption of Pb(II), Cd(II) and Ni(II) mixtures: Behavior and mechanism," *Ceramics International*, vol. 49, pp. 7030-7039, 2023. DOI:10.1016/j.ceramint.2022.10.164

[9] X. Peng, J. Yan, C. He, R. Liu and Y. Liu, "Sustainable triethylenetetramine modified sulfonated graphene oxide/chitosan composite for enhanced adsorption of Pb(II), Cd(II), and Ni(II) ions," *Journal of Molecular Liquids*, vol. 261, no 129741, 2024. DOI:10.1016/j.ijbiomac.2024.129741

[10] S. Khan, Z. Dan and H. Haiyan, "Adsorption mechanism of Pb(II) and Ni(II) from aqueous solution by TiO_2 nanoparticles: kinetics, isotherms and thermodynamic studies," *Desalination and Water Treatment*, vol. 155, pp. 237-249, 2019. DOI:10.5004/dwt.2019.23933

[11] M. Smith, B. Hamwi and R.E. Rogers, "Carbon nanomaterial-based aerogels for improved removal of copper(II), zinc(II), and lead(II) ions from water," *Environmental Science Advances*, vol. 1, pp. 208-215, 2022. DOI:10.1039/d2va00049k

[12] E.A. Al-Abbad and R.A. Al Dwairi, "Removal of nickel (II) ions from water by Jourdan natural zeolite as sorbent material," *Journal of Saudi Chemical Society*, vol. 25, no 101233. DOI:10.1016/j.jscs.2021.101233

[13] Z. Meng, J. Wu, S. Huang, L. Xin and Q. Zhoa, "Adsorption behaviors and mechanisms of Cd, Ni, and Cu by biochar when coexisting with microplastics under single, binary, and ternary systems," *Science of The Total Environment*, vol. 913, no 169524, 2024. DOI:10.1016/j.scitotenv.2023.169524

[14] A. Hashem, S.M. Badawy, S. Farag, L.A. Mohamed, A.J. Fletcher, G.M. Taha, "Non-linear adsorption characteristics of modified pine wood sawdust optimised for adsorption of Cd(II) from aqueous systems," *Journal of Environmental Chemical Engineering*, vol. 8, no 103966, 2020. DOI:10.1016/j.jece.2020.103966

[15] J.A. Álvarez-Álvarez, A. Aguilar-Aguilar, A. Robledo-Cabrera, R. Ocampo-Perez, R. Leyva-Ramos and E. Padilla-Ortega, "Contribution of halloysite as nanotubular clay mineral on mechanism and adsorption rate of Cd(II) onto nanocomposites alginate-halloysite," *Environmental Research*, vol. 216, no 114772, 2023. DOI:10.1016/j.envres.2022.114772

[16] S.M. Abdelbasir and M.A.A. Khalek, " From waste to waste: iron blast furnace slag for heavy metal ions removal from aqueous system," *Environmental Science and Pollution Research*, vol. 29, pp. 57964-57979, 2022. DOI:10.1007/s11356-022-19834-3

[17] S. Yasipourtehrani, V. Strezov, T. Kan and T. Evans, "Investigation of dye removal capability of blast furnace slag in wastewater treatment," *Sustainability*, vol. 13, pp. 1970-1986, 2021. DOI:10.3390/su13041970

[18] D. Zhao, Q. Qiu, Y. Wang, M. Huang, Y. Wu, X. Liu and T. Jiang, "Efficient removal of acid dye from aqueous solutions via adsorption using low-cost blast furnace slag," *Desalination and Water Treatment*, vol. 57, pp. 28486-28495, 2016, DOI:10.1080/19443994.2016.1179225

[19] C. Li, X. Li, Y. Yu, Q. Zhang, L. Li, H. Zhong and S. Wang, "A novel conversion for blast furnace slag (BFS) to the synthesis of hydroxyapatite-zeolite material and its evaluation of adsorption properties," *Journal of Industrial and Engineering Chemistry*, vol. 105, pp. 63-73, 2022. DOI:10.1016/j.jiec.2021.08.017

[20] A.S. Dhmees, N.M. Klaleel and S.A. Mahoud, "Synthesis of silica nanoparticles from blast furnace slag as cost-effective adsorbent for efficient azo-dye removal," *Egyptian Journal of Petroleum*, vol. 27, pp. 1113-1121, 2018. DOI:10.1016/j.ejpe.2018.03.012

[21] Le, Q.T.N., Vivas, E.L. and Cho, K. "Oxalated blast-furnace slag for the removal of Cobalt(II) ions from. aqueous solutions," *Journal of Industrial and Engineering Chemistry*, vol. 95, pp. 57-65, 2021. DOI:10.1016/j.jiec.2020.12.003

[22] C. X. Li, Q. W. Zhang and L. Li, "Synthesis of NaA Zeolite from Blast Furnace Slag (BFS) and Its Utilization for Adsorption of Basic Dye (Methylene Blue)," *Journal of Physics: Conference Series*, vol. 2224, no 012068, 2021, DOI:10.1088/1742-6596/2224/1/012068

[23] S.M. Abdel Moniem, R.M. Hegazey, M.A. Embaby, A.A. El-Kady and A.S. Dhmees, "Synthetic Zeolite from Blast Furnace Slag (BFS) as an effective sorbent for simultaneous removal of Cadmium and Copper ions," *Inorganic Chemistry Communications*, vol. 168, no 112870, 2024. DOI:10.1016/j.inoche.2024.112870.

[24] Y. Cheng, K. Wang, P. Li, H. Guo, B. Yan, D. Chen and W. Zhao, "A porous geopolymer containing Ti-bearing blast furnace slag: synthesis, characterization, and adsorption-photodegradation studies towards methylene blue removal under visible light condition," *Molecules*, vol. 28, pp. 3673-3690, 2023. DOI:10.3390/molecules28093673

[25] Y.L. Ni'mah, N.E. Yuningsih and S. Suprapto, "The Adsorption of Pb(II) Using Silica Gel Synthesized from Chemical Bottle Waste: Optimization Using Box-Behnken Design," *Journal of Renewable Materials*, vol. 11, pp. 2913-2924, 2023. DOI:10.32604/jrm.2023.025431

[26] M.R.A. Khadra, A.S. Mohamed, A.M. El-Sherbeeny and M.A. Elmeligy, "Enhanced photocatalytic degradation of acephate pesticide over MCM-41/Co_3O_4 nanocomposite synthesized from rice husk silica gel and peach leaves," *Journal of Hazardous Materials*, vol. 389, no 122129, 2020. DOI:10.1016/j.jhazmat.2020.122129

[27] N. Rahman, M. Nasir, P. Varshney, A.M. Al-Enizi, M.Ubaidillah, S.F. Shaikh and M.A. Al-Adrabalnabi, "Efficient removal of Pb(II) from water using silica gel functionalized with thiosalicylic acid: Response surface methodology for optimization," *Journal of King Saud University-Science*, vol. 33, no 101232, 2021. DOI:10.1016/j.jksus.2020.101232

[28] S.Y. Woo, H.S. Lee, H. Ji, D.S. Moon and Y.D. Kim, "Silica gel-based adsorption cooling cum desalination system: focus on brine salinity, operating pressure, and its effect on performance," *Desalination*, vol. 467, pp. 136-146, 2019. DOI:10.1016/j.desal.2019.06.016

[29] G. Gopikaa, K. Nithyab A. Sathisha, "Adsorption studies of amine-modified green synthesized Fe3O4 nanoparticles for the removal of nickel from aqueous solution," *Desalination and Water Treatment*, Vol. 121, pp. 53-64, 2018. DOI:10.5004/dwt.2018.22282

[30] K. Karami, S.M. Beram, P.Bayat, F. Siadatnasab, A. Ramezanpour, "A novel nanohybrid based on metal–organic framework MIL101-Cr/PANI/Ag for the adsorption of cationic methylene blue dye from aqueous solution," *Journal of Molecular Structure*, vol. 1247, no 131352, 2022. DOI:10.1016/j.molstruc.2021.131352

[31] A.I.A Sherlala, A.A.A Raman, M.M. Bello, A. Buthiyappan, "Adsorption of arsenic using chitosan magnetic graphene oxide nanocomposite," *Journal of Environmental Management*, vol. , 246, pp. 546-56, 2019, DOI:10.1016/j.jenvman.2019.05.117

[32] E.R. Nightingale Jr, "Phenomenological theory of ion solvation. Effective radii of hydrated ions," *Journal of Physical Chemistry*, vol. 63, pp. 1381-1387, 1959. DOI:10.1021/j150579a011.

[33] A. Drah, N.Z. Tomic, Z. Velicic, A.D. Marinkovic, Z. Radovanovic, Z. Velickovic, R. Jancic-Heinemann, "Highly ordered macroporous γ-alumina prepared by a modified sol-gel method with a PMMA microsphere template for enhanced Pb^{2+}, Ni^{2+} and Cd^{2+} removal," *Ceramics International*, vol. 43, pp. 13817-13827, 2017. DOI:10.1016/j.ceramint.2017.07.102

[34] A. Heidari, H. Younesi, Z. Mehraban, "Removal of Ni(II), Cd(II), and Pb(II) from a ternary aqueous solution by amino functionalized mesoporous and nanomesoporous silica," Chemical Engineering Journal, vol. 153, pp. 70-79, 2009. DOI:10.1016/j.cej.2009.06.016

[35] F.A. Razmi, N. Ngadi, S. Wong, I.M. Inuwa, L.A.Opotu, "Kinetics, thermodynamics, isotherm and regeneration analysis of chitosan modified pandan adsorbent," *Journal of Cleaner Production*, vol. 231, pp. 98-109, 2019. DOI:10.1016/j.jclepro.2019.05.228

[36] K. Rambabu, G. Bharath, F. Banat, P.L. "Show biosorption performance of date palm empty fruit bunch wastes for toxic hexavalent chromium removal," *Environmental Research*, vol. 187, no 109694, 2020, DOI:10.1016/j.envres.2020.109694

[37] C.S.T. Araújo, I.L.S. Almeida, H.C. Rezende, S.M.L.O. Marcionilio, J.J.L. Léon, T.N.de Matos, "Elucidation of mechanism involved in adsorption of Pb(II) onto lobeira fruit (Solanum lycocarpum) using Langmuir, Freundlich and Temkin isotherms," *Microchemical Journal*, vol. 137, pp. 348-354, 2018. DOI:10.1016/j.microc.2017.11.009

[38] D. E. AL-Mammar, "Adsorption of brilliant scarlet 3r dye onto corn silkas agricultural waste in neutral medium," *Iraqi Journal of Science*, vol. 65, no 7, pp. 3606-3619, 2024. DOI:10.24996/ijs.2024.65.7.3

[39] N.H. Ibrahim, S.M. Al-Jubour, "Green porous composite for combining ion exchange-adsorptive removal of zinc ions from aqueous solutions," *Iraqi Journal of Science*, 2024, vol. 65, pp. 6229-6241, 2024. DOI:10.24996/ijs.2024.65.11.3